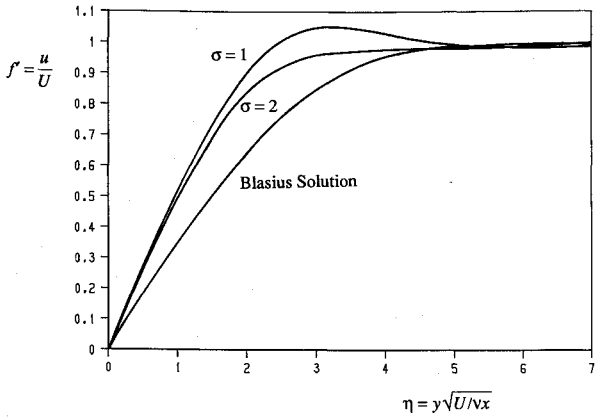

Fig. 3 Effect of the wave parameter and Strouhal number on time-mean velocity profiles.

ing rise to a computational procedure that is able to account for the effect of so-called "wake-passing" on the laminar boundary layer. A similar computational procedure, which is efficient and may be readily incorporated into existing boundary-layer codes, has been developed by Greenblatt[6] for standing-wave-type disturbances. In the light of recent attention that has been given to the effect of wake-passing on boundary layer transition,[5] a code that can predict the effect of wake-passing on the laminar boundary layer will compliment these developments. The authors believe that the work presented in this Note lays important elements of the foundation for such a code.

Conclusions

In this Note, the effect of high-frequency traveling-wave fluctuations on a flat-plate boundary layer was considered. The analysis yielded useful engineering correlations based on the dimensionless wave parameter $\Gamma (\equiv \varepsilon^2\sigma/\gamma)$ and the Strouhal number σ. It was shown that Γ has a pronounced effect on both the local skin-friction coefficient and the momentum thickness, whereas σ only affects the momentum thickness significantly. It was suggested that the traveling wave phenomenon should be considered when studying the complicated problem of transition onset.

Acknowledgment

The first author would like to thank the members of the Turbomachinery Program and the Computational Fluid Dynamics Facility at Aerotek for their many useful comments and constructive criticisms.

References

[1]Evans, R. L., "Turbulence and Unsteadiness Measurements Downstream of a Moving Blade Row," *ASME Journal of Engineering For Power,* Vol. 100, Jan. 1975, pp. 131–139.

[2]Graham, R. W., "Fundamental Mechanisms that Influence the Estimate of Heat Transfer to Gas Turbine Blades," ASME/AIChE 18th National Heat Transfer Conference (San Diego, CA), American Society of Mechanical Engineers, Paper 79-HT-43, 1979.

[3]Schlichting, H., *Boundary Layer Theory,* McGraw-Hill, New York, 1979, Chaps. 7 and 15.

[4]Evans, R. L., "Computation of Unsteady Laminar Boundary Layers Subject to Traveling-Wave Freestream Fluctuations," *AIAA Journal,* Vol. 27, No. 11, 1989, pp. 1644–1646.

[5]Mayle, R. E., "The Role of Laminar-Turbulent Transition in Gas Turbine Engines," ASME IGTI Scholar Lecture, *ASME Journal of Turbomachinery,* Vol. 113, Oct. 1991, pp. 509–537.

[6]Greenblatt, D., "The Combined Effect of Unsteady Freestream Velocity and Freestream Turbulence on Heat Transfer to Gas Turbine Blades," *Tenth International Symposium on Air Breathing Engines,* edited by F. S. Billig, Vol. 2, Nottingham, England, UK, 1991, pp. 1285–1290.

TURNS: A Free-Wake Euler/Navier-Stokes Numerical Method for Helicopter Rotors

G. R. Srinivasan* and J. D. Baeder†
NASA Ames Research Center,
Moffett Field, California 94035

Introduction

THE accurate prediction of the aerodynamic flowfield, including the acoustics of a helicopter rotor, continues to be a complex and challenging problem despite the availability of modern supercomputers and improved numerical methods. This complexity stems from several peculiar features unique to helicopter rotors. Of these, the vortical wake plays a dominant role since it is largely responsible for unsteady load fluctuation, noise, and vibration. Also, it is the most difficult component of the flowfield to accurately predict.[1] Radiated noise can severely restrict rotorcraft usage in both civilian and military operations. Impulsive noise, the sum total of the blade-vortex interaction (BVI) noise and high-speed impulsive (HSI) noise, forms the most important component of the radiated noise. The BVI noise is generated due to the interaction of the vortical wake with the rotating blades and is generally more difficult to model due to the importance of unsteady, three-dimensional, and wake effects. HSI noise, on the other hand, is caused primarily by compressibility effects. If the advancing blade tip Mach number is highly supercritical, the phenomenon known as delocalization may occur, whereby the supersonic pocket on the rotor blade extends out to the farfield beyond the blade tip. If this occurs, the noise becomes more impulsive and, in particular, gets focused in its direction of propagation. Fortunately, the influence of lift on HSI noise appears to be secondary.[2] Thus, one can estimate this even with nonlifting configurations.

Recent studies using the Euler and Navier-Stokes methods have demonstrated the feasibility of using a single computational fluid dynamics (CFD) method to calculate simultaneously the aerodynamics and acoustics of a helicopter rotor in hover and forward flight.[3-5] This Note summarizes the computational capabilities of a numerical procedure, called TURNS[5] (transonic unsteady rotor Navier-Stokes), to calculate the aerodynamics and acoustics (HSI) out to several rotor diameters, all in one single solution without using any modeling either for wake or acoustic propagation. The vortical wake and its influence, as well as the acoustics, are captured as a part of the overall flowfield solution. Comparisons of the numerical results with the available experimental data demonstrate the accuracy and suitability of this method.

Numerical Method

The choice of govering equations affects the level of physics modeled and computational time. In this study, the unsteady Euler/Navier-Stokes equations are preferred to accurately model strong shocks and accompanying HSI noise, viscous-inviscid interaction, the flow in the tip region where the tip vortex forms, and the vortical wake. The Navier-Stokes equations are considered in the thin-layer approximation and an algebraic turbulence model[6] is used to obtain estimates of eddy viscosity for calculating turbulent flows. The govering equa-

Received Aug. 22, 1992; revision received Sept. 28, 1992; accepted for publication Sept. 28, 1992. This paper is declared a work of the U.S. Government and is not subject to copyright protection in the United States.

*Senior Staff Scientist, JAI Associates, Inc., P. O. Box 293, Mt. View, CA 94042. Associate Fellow AIAA.

†Research Scientist, U.S. Army Aeroflightdynamics Directorate-ATCOM. Member AIAA.

tions and finite-difference, implicit numerical scheme are described elsewhere.[5] The hovering cases are calculated in a blade-fixed reference frame, whereas the forward-flight cases are calculated in the inertial reference system. The details of body-conforming grid generation to capture the details of the flowfield, including acoustics propagation as well as the boundary conditions procedure, are discussed in Refs. 3–5. Typical grids have 100,000 to 960,000 grid points, with a spacing at the surface in the normal direction of 0.00004 chord for the fine grids. Finally, to take advantage of the symmetry of the flowfield from blade to blade in the hovering configuration, flowfield computations are performed on an isolated rotor blade by using the information from the neighboring blade through a periodic boundary condition procedure.[5]

Results and Discussion

In this section, both quasisteady (hover) and unsteady (forward-flight) numerical results are presented and compared with experimental data for a rotor-only configuration. Several test conditions from among many model rotor experiments are selected for computations. The forward-flight BVI calculations are done first for a nonlifting rotor in the absence of vortex interaction. These results are then used as the baseline solution for calculating a lifting, three-dimensional blade-vortex interaction flowfield. All acoustic (HSI) calculations reported here are done for nonlifting rotor configurations; to take advantage of the symmetry of the flow, only one-half of the plane of the rotor blade is used.

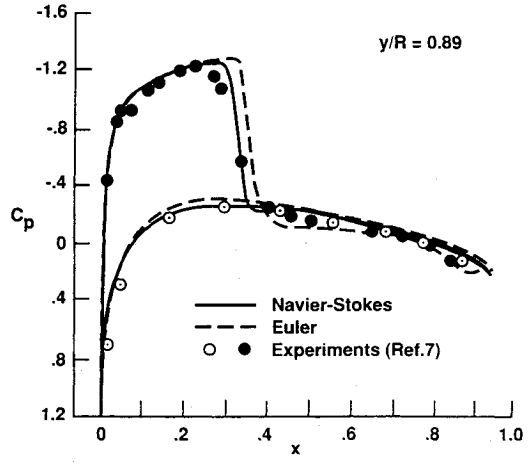

Fig. 1 Comparison of surface pressures for a lifting two-bladed rotor in hover. $M_{tip} = 0.877$, $\theta_c = 8$ deg, and $Re = 3.93 \times 10^6$.

Rotor in Hover

The model rotor test cases chosen for calculating the aerodynamic flowfield correspond to the several lifting configurations of a two-bladed rotor.[7] Figure 1 shows a typical result of surface pressures C_p at one radial station, $r/R = 0.89$, for the test condition of tip Mach number of $M_{tip} = 0.877$, collective pitch of $\theta_c = 8$ deg, and Reynolds number of $Re = 3.93 \times 10^6$. Here, r is the radial coordinate of the blade and R the radius of the rotor. As seen in this figure, the numerical results are in good agreement with experiments. The shock wave location and strength are overpredicted with the Euler method, as expected. The calculations show that the near wake trajectory and its influence are well captured, although its structure is diffused. It appears that the airloads are influenced more by the nearfield wake effects. The use of the periodicity condition provides the necessary vortical wake information of other blades of the rotor and hence no additional wake information has to be supplied externally. The farfield boundary conditions play an important role in calculating the correct wake trajectory as it descends down the rotor and exits at the farfield boundary. This aspect of the numerical procedure needed special attention and has been described in Ref. 8.

For calculating the HSI noise, the rotor blade considered is from the experiments of Ref. 9. The blade is a 1/7th scale model of a UH-1H main rotor with untwisted rectangular blades of NACA 0012 airfoil section. This rotor has an aspect ratio of 13.7. The computations were done on a $49 \times 37 \times 55$ grid (half-plane) with a grid boundary located 48 chords away from the center of rotation. The first case examined is $M_{tip} = 0.90$ and $Re = 1.6 \times 10^6$ for which the flow is just delocalized. The pressure time histories at 3.09 rotor radii are shown in Fig. 2a. The predicted amplitude of the negative peak pressure, as well as the wave shape, agrees well with experiments. Similar agreement occurs at other locations also. For this weak shock case, the Euler and Navier-Stokes results are nearly identical. In contrast to the present CFD method, studies using the acoustic analogy method[2] or nonlinear Kirchoff formulation,[10] with aerodynamic input from either a small disturbance code or full potential code, underpredict the negative peak pressure.

If M_{tip} is increased to 0.95, the shock on the surface of the blade becomes very strong. Examination of the pressure con-

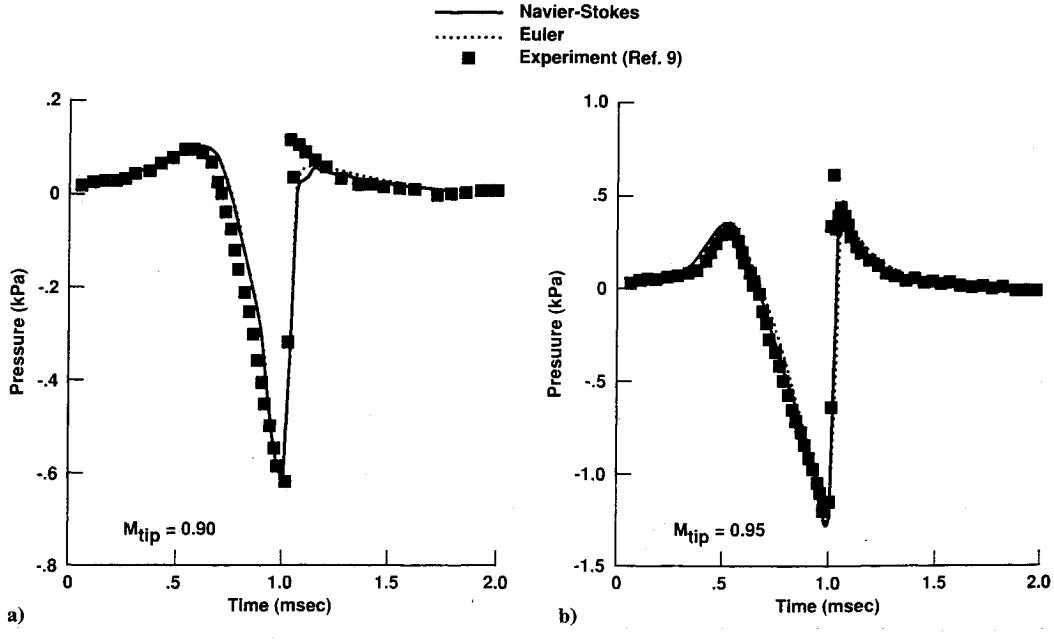

Fig. 2 Pressure time histories of HSI noise in-plane at $r/R = 3.09$ for a rectangular blade rotor in hover a) at $M_{tip} = 0.90$ and b) at $M_{tip} = 0.95$.

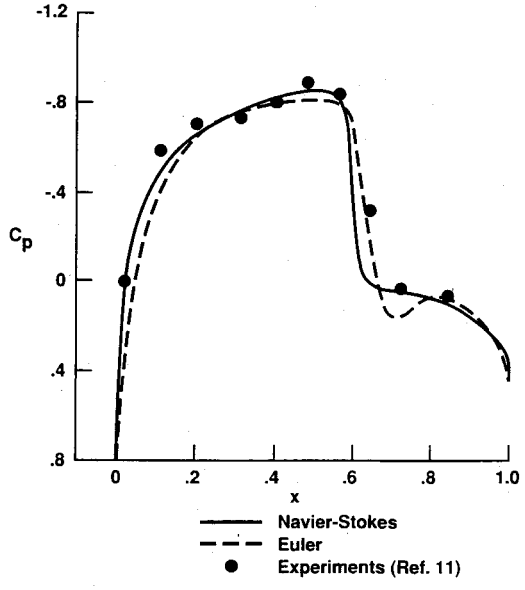

Fig. 3 Instantaneous surface pressure distribution of a nonlifting rotor in forward flight at $\Psi = 120$ deg azimuth compared with experiments. $M_{tip} = 0.8$, $\mu = 0.2$, $Re = 2.89 \times 10^6$, and $r/R = 0.893$.

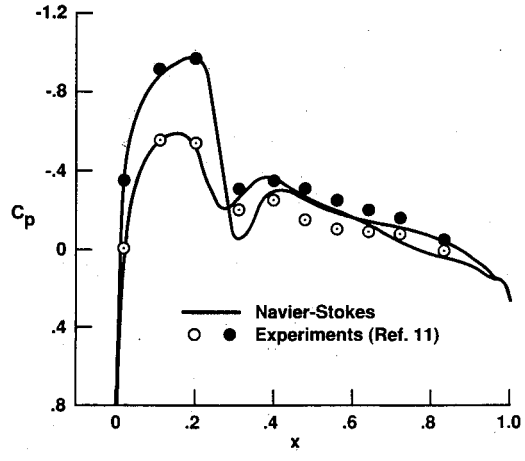

Fig. 4 Instantaneous surface pressures during transonic parallel BVI at $\Psi = 174.5$ deg azimuth compared with experiments. $M_{tip} = 0.8$, $\mu = 0.2$, $\bar{\Gamma} = 0.177$, $x_0 = 0.0$, $z_0 = -0.4$, and $r/R = 0.893$.

tours, in a plane normal to the blade surface at 98% of the span, indicates that the Navier-Stokes results show the shock location slightly upstream and more smeared at its root than the Euler results. However, away from the blade surface the shock location and strength appear to be nearly identical to those of the Euler results. The resulting pressure time histories at 3.09 rotor radii are shown in Fig. 2b. Again, the agreement with experiment is excellent. The reason for the overall good agreement of the Euler results with those of Navier-Stokes is that HSI noise is caused by the (summation of the) large gradients across the whole flowfield, not just the portion of the shock that intersects the blade surface.

Rotor in Forward Flight

The two-bladed rigid rotor considered here for flowfield calculation is a nonlifting configuration. However, the interaction of this rotor with an externally generated line vortex[11] generates lift on the rotor blade. Several test calculations have been performed corresponding to the model rotor test conditions.[11,12] Typical results of instantaneous surface pressures for the conditions of $M_{tip} = 0.8$ and advance ratio $\mu = 0.2$, and

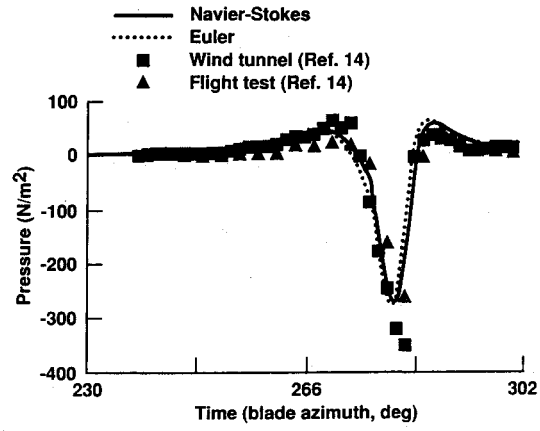

Fig. 5 Pressure time histories of HSI noise in-plane at 1.8 rotor diameters directly in front of the blade for an advancing blade tip Mach number of $M_{tip} = 0.896$, $\mu = 0.348$, and $Re = 2.17 \times 10^6$ compared to wind-tunnel and flight-test data.

in the absence of vortex interaction, are shown in Fig. 3 for an azimuthal location, $\Psi = 120$ deg, of the blade in the advancing cycle. Both the Euler and Navier-Stokes results show good agreement with experiments for the surface pressures; the Euler calculations overpredict the shock location and strength. With this baseline solution, a vortex-fitting technique[13] is used to introduce the convecting vortex flowfield into the rotor flowfield and the interaction flowfield is then calculated. The interacting line vortex lies along the y axis and is located at $x_0 = 0.0$ and $z_0 = -0.4$, where x, y, and z are the physical space coordinates. These are, respectively, along the chord of the blade, along the radius of the blade, and normal to the blade surface. Both parallel and oblique blade-vortex interactions have been calculated for several tip Mach numbers. In contrast to the subcritical flow conditions, the presence of shock waves under supercritical flow conditions appears to enhance the flow unsteadiness and three-dimensionality. A typical result of instantaneous surface pressure distribution for a parallel blade-vortex interaction, calculated on a coarse grid, is shown in Fig. 4, along with a comparison to experimental data. For this azimuthal position of the blade, $\Psi = 174.5$ deg, the BVI has peaked. As seen, the results are in fair agreement with experiments. Although not shown here, the oblique BVI occurs over a larger azimuthal travel of the blade. The interaction begins in the first quadrant and is completed only toward the end of the second quadrant.

For calculating the HSI and its propagation, the OLS rotor blade of an AH-1 helicopter is selected due to its simple geometry of a rectangular planform with constant thickness. The maximum thickness of the airfoil is 9.71% chord and the rotor blade has an aspect ratio of 9.22. Acoustic data are available for full-scale and model OLS blades.[14] For the calculations reported here, the twist of the blade is neglected and the tip-path plane angle and collective pitch are set to zero. The mesh consists of $73 \times 55 \times 55$ points with 55×19 points on the blade, covering the upper half-plane of the whole flowfield.

The test case examined is for $M_{tip} = 0.665$, an advance ratio $\mu = 0.348$, and $Re = 2.17 \times 10^6$. The flowfield is delocalized[2] for a short period of time. The time histories of the pressure pulse at 1.8 rotor diameters directly in front of the blade are shown in Fig. 5. Nonlinear effects manifest themselves in the steeper compression wave and magnitude of the pulse; calculations using linear theory underpredict the negative peak pressure.[3] A detailed examination of the Euler and Navier-Stokes solutions reveals strong directivity. The propagated noise to the sides of the blade is relatively small and nonimpulsive. Upstream of the rotor, however, the propagated noise is very large and impulsive. Similar trends have been observed in experiments. Further examination of the pressure contours in the plane of the rotor shows the growth and decay of the

supersonic pocket on the rotor blade surface, the initial separation of the acoustic wave from the aerodynamic field, and the propagation of the acoustic wave to the farfield. It is currently impossible to obtain such detailed information from experiments.

Conclusions

This study demonstrates the capabilities of a free-wake Euler and Navier-Stokes CFD methodology, called TURNS, in calculating helicopter rotor aerodynamic flowfields, including the acoustics (high-speed impulsive noise), in both hover and forward flight. The aerodynamics and acoustics information can be obtained in one single calculation. Agreement with experiments is very encouraging, demonstrating the ability of the solution scheme to capture the flowfield and acoustic details that are hard to obtain from experiments.

Acknowledgments

The authors would like to thank W. J. McCroskey for his encouragement and continued interest. The first author would like to acknowledge the research support from the U. S. Army Research Office under Contract DAAL03-90-C-0013.

References

[1]McCroskey, W. J., "Special Opportunities in Helicopter Aerodynamics," *Recent Advances in Aerodynamics,* edited by A. Krothapalli and C. A. Smith, Springer-Verlag, New York, 1986, pp. 721–752.

[2]Schmitz, F. H., and Yu, Y. H., "Helicopter Impulsive Noise: Theoretical and Experimental Status," *Recent Advances in Aeroacoustics,* edited by A. Krothapalli and C. A. Smith, Springer-Verlag, New York, 1986, pp. 149–243.

[3]Srinivasan, G. R., and Baeder, J. D., "Recent Advances in Euler and Navier-Stokes Methods for Calculating Helicopter Rotor Aerodynamics and Acoustics," *Proceedings of the Fourth International Symposium on Computational Fluid Dynamics* (Davis, CA), Sept. 1991, pp. 1095–1100.

[4]Baeder, J. D., "Euler Solutions to Nonlinear Acoustics of Non-Lifting Rotor Blades in Forward Flight," paper presented at the American Helicopter Society-Royal Aeronautical Society International Technical Specialists Meeting on Rotorcraft Acoustics and Rotor Fluid Dynamics (Philadelphia, PA), Oct. 1991.

[5]Srinivasan, G. R., Baeder, J. D., Obayashi, S., and McCroskey, W. J., "Flowfield of a Lifting Rotor in Hover—A Navier-Stokes Simulation," *AIAA Journal,* Vol. 30, No. 10, 1992, pp. 2371–2378.

[6]Baldwin, B. S., and Lomax, H., "Thin Layer Approximation and Algebraic Model for Separated Turbulent Flow," AIAA Paper 78-0257, Jan. 1978.

[7]Caradonna, F. X., and Tung, C., "Experimental and Analytical Studies of a Model Helicopter Rotor in Hover," NASA TM-81232, Sept. 1981.

[8]Srinivasan, G. R., Raghavan, V., and Duque, E. P. N., "Flowfield Analysis of Modern Helicopter Rotors in Hover by Navier-Stokes Method," Paper presented at the American Helicopter Society-Royal Aeronautical Society International Technical Specialists Meeting on Rotorcraft Acoustics and Rotor Fluid Dynamics (Philadelphia, PA), Oct. 1991.

[9]Boxwell, D. A., Yu, Y. H., and Schmitz, F. H., "Hovering Impulsive Noise: Some Measured and Calculated Results," *Vertica,* Vol. 3, No. 1, 1979, pp. 35–45.

[10]Purcell, T. W., "A Prediction of High Speed Rotor Noise," AIAA Paper 89-1130, July 1989.

[11]Caradonna, F. X., Laub, G. H., and Tung, C., "An Experimental Investigation of the Parallel Blade-Vortex Interaction," Paper No. 4, *Proceedings of the Tenth European Rotorcraft Forum* (The Hague, The Netherlands), Aug. 1984.

[12]Caradonna, F. X., Lautenschlager, J. L., and Silva, M. J., "An Experimental Study of Rotor-Vortex Interactions," AIAA Paper 88-0045, Jan. 1988.

[13]Srinivasan, G. R., McCroskey, W. J., and Baeder, J. D., "Aerodynamics of Two-Dimensional Blade-Vortex Interaction," *AIAA Journal,* Vol. 24, No. 10, 1986, pp. 1569–1576.

[14]Schmitz, F. H., Boxwell, D. A., Splettstoesser, W. R., and Schultz, K. J., "Model Rotor High-Speed Impulsive Noise: Full-Scale Comparisons and Parametric Variations," *Vertica,* Vol. 8, No. 4, 1984, pp. 395–422.

Correlation of Conical Interactions Induced by Sharp Fins and Semicones

Xue-Ying Deng* and Jin Hua Liao†
Beijing University of Aeronautics and Astronautics, Beijing 100083, People's Republic of China

Introduction

The conical interactions are one important type of swept shock wave and boundary-layer interactions and have been extensively studied.[1,2] Most research has studied the conical interaction behaviors induced by individual shock generators such as swept compression corner, sharp fin, semicone, and so on.[1,2] However, their correlative behaviors—which means their common interaction features induced by dissimilar shock generators—have been less studied. Settles and Lu[3] were the first to make conical correlation induced by unswept sharp fins and swept sharpfins at M_∞ = 2.95. Settles and Kimmel[4] also tried to correlate quasiconical interaction behaviors generated by four types of dissimilar shock generators at M_∞ = 2.95. This Note studies the correlative behaviors induced by sharp fins and semicones and extends the previous conical similarity to the condition of varying freestream Mach number, especially in the low Mach number range. Furthermore, it demonstrates that the inviscid shock strength is a dominant parameter for the conical interactions.

Experimental Procedures

All tests were carried out in a G-3 supersonic wind tunnel with a test section of 54.8 × 47.0 cm^2 at Beijing University of Aeronautics and Astronautics (BUAA). A flat plate of 54.6 × 90 cm^2 was mounted in the test section horizontally, and the sharp fin or semicone model was attached to it. Tests were conducted at M_∞ = 1.79, 2.04, and 2.50, keeping the same Reynolds number $Re = 2.4 \times 10^7$/m. The boundary layer on the plate was tripped by the sand band with sand size of 80#. And this sand band with a 3 mm width is attached on the plate 5 mm from the leading edge of the plate. The fin and semicone models were placed 650 mm from the model apex to the leading edge of the plate. Undisturbed boundary-layer profiles in the test region were surveyed along the plate centerline using Sun-Childs wall-wake[5] curvefit to the survey data. And these survey results showed[6] that those profiles agree with wall-wake law well with a wake strength of π = 0.55 ~ 0.67. The incoming boundary layer overall, displacement, and momentum thicknesses at the position 650 mm from the leading edge of the plate were 9.41 ~ 9.39 mm, 1.97 ~ 2.35 mm, 0.68 ~ 0.59 mm, respectively, for the test Mach numbers.

The sharp fin model was tested at angles of attack 6, 8, 10, 12, 16, and 20 deg for all Mach numbers, except the largest angle at M_∞ = 1.79 was limited by tunnel stall. Three semicone models with half-angles of 20, 25, and 30 deg were tested.

The present experiments consider the mean footprints of three-dimensional interactions as revealed by the kerosene-lampblack streak method. The upstream influence line and primary separation line in the interaction region can be detected from it.

Results and Discussion

A typical surface flow pattern of interaction with sharp fin or semicone is sketched in Fig. 1. It shows the conical symmetry feature for both shock generators. To select the flow region to be correlated with both shock generators, their inviscid flowfields might be considered. Both inviscid flow patterns downstream of the

Presented as Paper 91-1756 at the AIAA 22nd Fluid Dynamics, Plasma Dynamics, and Lasers Conference, Honolulu, HI, June 24–26, 1991; received July 26, 1991; revision received Aug. 3, 1992; accepted for publication Aug. 17, 1992.

*Professor, Fluid Mechanics Institute. Member AIAA.
†Graduate Student, Fluid Mechanics Institute.